Fitton, J.G., Mahoney, J.J., Wallace, P.J., and Saunders, A.D. (Eds.)
Proceedings of the Ocean Drilling Program, Scientific Results Volume 192

2. Apparent Cooling in the Tropical Pacific during the Maastrichtian and Diagenetic Artifacts in Late Cretaceous Stable Isotopic Trends in Bulk Carbonate from Ontong Java Plateau[1]

Kenneth G. MacLeod[2] and J.A. Bergen[3]

ABSTRACT

Stable isotopic analyses of bulk carbonates recovered from Ontong Java Plateau during Ocean Drilling Program (ODP) Leg 192 (Holes 1183A and 1186A) show an ~0.5‰ increase in $\delta^{18}O$ values from the upper Campanian/lower Maastrichtian to the upper Maastrichtian. This shift is consistent with widespread evidence for cooling at this time. Similar shifts were found at other localities on Ontong Java Plateau (Deep Sea Drilling Project [DSDP] Sites 288 and 289 and ODP Site 807) and at DSDP Site 317 on Manihiki Plateau. These data extend evidence for Maastrichtian cooling into the southwestern tropical and subtropical Pacific. The record of apparent cooling survives despite a significant diagenetic overprint at all sites. Comparing average Maastrichtian $\delta^{18}O$ values among sites suggests that diagenesis caused $\delta^{18}O$ to first be shifted toward higher values and then back toward lower values as burial depth increased. Carbon isotopes at the six sites show no apparent primary shifts, but at four sites, the Cretaceous/Tertiary boundary interval coincides with a negative excursion attributed to alteration of sediments near the boundary.

[1]MacLeod, K.G., and Bergen, J.A., 2004. Apparent cooling in the tropical Pacific during the Maastrichtian and diagenetic artifacts in Late Cretaceous stable isotopic trends in bulk carbonate from Ontong Java Plateau. *In* Fitton, J.G., Mahoney, J.J., Wallace, P.J., and Saunders, A.D. (Eds.), *Proc. ODP, Sci. Results,* 192, 1–15 [Online]. Available from World Wide Web: <http://www-odp.tamu.edu/publications/192_SR/VOLUME/CHAPTERS/108.PDF>. [Cited YYYY-MM-DD]
[2]Department of Geological Sciences, University of Missouri, Columbia MO 65211-1380, USA.
macleodk@missouri.edu
[3]BP America, 501 Westlake Park Boulevard, Houston TX 77079, USA.

Initial receipt: 31 July 2003
Acceptance: 29 January 2004
Web publication: ## Month 2004
Ms 192SR-108

INTRODUCTION

The Campanian and Maastrichtian sequence on Ontong Java Plateau (OJP) presents many frustrations for paleoceanographic study, but it also provides a view on conditions in a portion of the Cretaceous tropical to subtropical Pacific for which better samples are not available. Frustrations include coring gaps, deep burial, and high degrees of lithification. However, the presence of multiple holes in the same region increases the available record and allows comparison of patterns within and among sites so that paleoceanographic and diagenetic signals can begin to be separated. Trends repeated at all sites despite different burial histories likely reflect paleoceanographic events. Differences in values or trends among sites could represent local signals. Especially where they depart from expected paleoceanographic values, though, they are more conservatively interpreted as the result of alteration. As such, these differences can be used to estimate the direction and magnitude of diagenetic overprints.

MATERIALS AND METHODS

This paper presents stable isotopic data for bulk samples from the western Pacific with an emphasis on the Campanian and Maastrichtian record in Ocean Drilling Program (ODP) Holes 1183A and 1186A. These sites are on OJP and were recovered during ODP Leg 192. In addition, five other holes from OJP (Deep Sea Drilling Project [DSDP] Holes 288A and 289 and ODP Holes 807C, 1184A, and 1185A) and one hole from Manihiki Plateau (DSDP Hole 317A) were examined. The sections are dominated by chalk and limestone with chert interbeds (Andrews, Packham, et al., 1975; Schlanger, Jackson, et al., 1976; Kroenke, Berger, Janacek, et al., 1991; Mahoney, Fitton, Wallace, et al., 2001). Calcareous nannofossils, foraminifers, and radiolarians are the dominant sediment sources at all sites. Terrigenous material is a minor component, and the limestones are consistently >90 wt% and generally >95 wt% calcium carbonate. Estimated Late Cretaceous paleolatitudes range from ~15° to ~30°S (Fig. **F1**); burial depths range from <600 m in Hole 317A and the upper Maastrichtian in Hole 288A to >1300 m for the upper Campanian in Hole 807C (Andrews, Packham, et al., 1975; Schlanger, Jackson, et al., 1976; Kroenke, Berger, Janacek, et al., 1991; Mahoney, Fitton, Wallace, et al., 2001). Backtracking current bathymetry, taking into consideration expected subsidence related to the cooling of the igneous pile and to the weight and compaction of the sedimentary cover, suggests Maastrichtian water depths ranged from ~2000 to >3000 m (J. Ogg et al., unpubl. data).

Bulk samples were collected from the Maastrichtian to Campanian from six DSDP/ODP Holes (288A, 289, 317, 807C, 1183A, and 1186A). Sampling density is greatest in Holes 807C, 1183A, and 1186A, where a relatively even distribution of samples across the Campanian–Maastrichtian interval is available. Stratigraphic coverage was enhanced by analyzing carbonate-bearing residues of Cretaceous and Tertiary samples from Leg 192 shipboard X-ray diffraction (XRD) studies. Comparable results spanning the Neogene–Albian are available for Hole 807C (Corfield and Cartlidge, 1993). An ~1-g portion of each bulk sample was cleaned ultrasonically under distilled deionized water, dried at <50°C, and powdered with an agate mortar and pestle. Preparation of

F1. Paleogeographic map, p. 9.

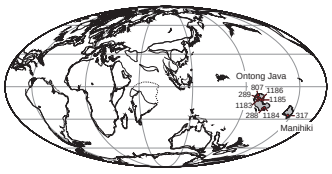

samples for Leg 192 shipboard XRD analysis was similar (Mahoney, Fitton, Wallace, et al., 2001).

A 50- to 100-µg separate of each powder was loaded into an individual reaction vial, and its $\delta^{13}C$ and $\delta^{18}O$ values were measured in the Biogeochemistry Isotope Laboratory at the University of Missouri. Samples were reacted at 70°C in 100% H_3PO_4 on a Kiel III carbonate device. The evolved CO_2 was cryogenically distilled, and its isotopic composition was measured online using a Finnigan MAT DeltaPlus isotope ratio mass spectrometer. Results are reported in standard delta notation relative to the Vienna Peedee Belemnite (VPDB) standard. The instrument is calibrated for each run based on the average of multiple analyses of NBS-19 standard. External precision of the instrument through the duration of this study was <0.03‰ for $\delta^{13}C$ and <0.05‰ for $\delta^{18}O$ (1 σ, standard deviation).

Age estimates are based on nannofossils and Sr isotope stratigraphy. For Holes 1183A and 1186A, ages estimated from $^{87}Sr/^{86}Sr$ ratios measured on a subset of the bulk samples are in good agreement with Campanian–Maastrichtian biostratigraphy (**Bralower et al.,** this volume). To construct age models for these holes, $^{87}Sr/^{86}Sr$ ratios were converted to age using tables from McArthur et al. (2001) after adjusting the OJP data by –0.0000175. This adjustment was proposed as an empirical correction for interlaboratory differences (MacLeod et al., 2003) but may reflect age differences in the datums used to project the stratigraphy onto the geologic timescale (**Bralower et al.,** this volume). The Sr age model for each site is a linear fit to the resulting age/depth plot, and these fits are statistically excellent (Fig. **F2**). Nannofossil datums are used to tie Leg 192 holes to the other four holes studied (Table **T1**). Ages for the intervals between the biostratigraphic tie points in the other four holes are interpolated.

RESULTS

Trends in isotopic values through the Campanian–Maastrichtian sections recovered in Holes 1183A and 1186A are quite similar (Figs. **F3, F4;** Table **T2**). In both holes, $\delta^{18}O$ values are 0.5‰–1.0‰ lower in upper Campanian–lower Maastrichtian samples than in the upper Maastrichtian samples and the rate of change is most rapid in the middle portion of the Maastrichtian. Further, in both holes $\delta^{13}C$ values are near $3‰_{VPDB}$ throughout most of the Campanian–Maastrichtian with an excursion near the Cretaceous/Tertiary (K/T) boundary. In Hole 1183A, $\delta^{13}C$ values exhibit a negative excursion of ~1.5‰ across ~10 m of section spanning the youngest Cretaceous and oldest Paleogene rocks, whereas in Hole 1186A, the oldest Paleogene sample has a $\delta^{13}C$ value ~1.5‰ lower than the youngest Cretaceous samples (Fig. **F3**). Aptian–Campanian powders (XRD residues) were also analyzed from Hole 1183A. In the middle Campanian (~1080–1100 meters below seafloor [mbsf]) $\delta^{18}O$ values are lower than in the Maastrichtian. Both $\delta^{13}C$ and $\delta^{18}O$ values are relatively high in Aptian–Albian samples (~1100–1140 mbsf), which are near the basalt/sediment contact. The one comparable sample from near the sediment/basalt contact in Hole 1186A (upper Aptian; 948.55 mbsf) also shows relatively high $\delta^{13}C$ and $\delta^{18}O$ values.

In younger samples from OJP, there is a general trend toward higher $\delta^{18}O$ values upsection consistent with the long-term cooling during the Cenozoic (Fig. **F3**). Samples from Holes 1183A and 1186A both show a

F2. Age-depth plots, p. 10.

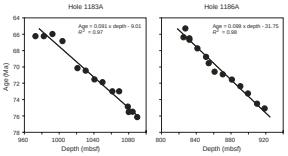

T1. Nannofossil datum levels used for correlation, p. 13.

F3. Plots of isotopic values, p. 11.

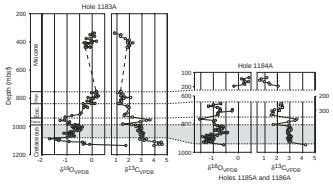

F4. Oxygen and carbon isotopic plots, p. 12.

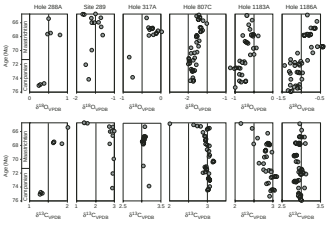

T2. Stable isotopic values of bulk samples, p. 14.

prominent positive excursion in $\delta^{13}C$ in the Paleocene that seems to correspond to the late Paleocene excursion in the compilation of Zachos et al. (2001). This feature as well as the trend toward higher $\delta^{18}O$ values upsection was previously observed in Hole 807C (Corfield and Cartlidge, 1993). That study documented the Tertiary record on OJP in greater detail than provided by our analyses of the XRD residues and, thus, the Tertiary record is not discussed further here.

Features in the isotopic curves for the Campanian–Maastrichtian interval in Holes 1183A and 1186A seem to be supported at each of the other four sites (Fig. F4). Average $\delta^{18}O$ values for Campanian–Maastrichtian samples vary from –1.8‰$_{VPDB}$ (Hole 807C) to 0.5‰$_{VPDB}$ (Hole 288A) among the holes, but in each hole there is an upsection increase of 0.5‰–1.0‰ within the Maastrichtian. Further, $\delta^{13}C$ values in Holes 289, 317A, 807C, 1183A, and 1186A are near 3‰$_{VPDB}$ across most of the Campanian–Maastrichtian interval, although in Hole 288A $\delta^{13}C$ values average 1.6‰$_{VPDB}$ and appear to increase through the Maastrichtian. Finally, data for Holes 289 and 807C show an ~1.5‰ decrease in $\delta^{13}C$ just below the K/T boundary (Fig. F4), similar to the record in Hole 1183A.

DISCUSSION

The most likely candidate for a paleoceanographic signal in the bulk isotopic data is the increase in $\delta^{18}O$ values in the middle portion of the Maastrichtian. The shift occurs within the same relatively narrow stratigraphic interval (equivalent to ~69–70 Ma with the age model used) at all six sites despite the fact that burial depths range from <600 m to >1300 m among the sites analyzed.

The consistent stratigraphic position argues that the shift at least partially reflects conditions at the time of deposition. That is, it is not simply a diagenetic effect related to burial and separate from paleoceanography. However, in Hole 1183A the shift corresponds to the level at which the quality of preservation changes, and in Hole 1186A the shift corresponds to the level at which the foraminiferal lysocline was crossed (P. Sikora and J. Ogg, unpubl. data). Poorer preservation in older samples might introduce a bias at all six sites studied, but the preservational changes are not the same at all sites. Further, the shift is in the opposite direction from what would be expected if dissolution preferentially removed material precipitated in warm surface water and was, thus, most out of equilibrium with bottom water. That said, the correlation between preservational evidence for Maastrichtian changes in the depth of the lysocline and carbonate compensation depth on OJP (J. Ogg et al., unpubl. data; P. Sikora and J. Ogg, unpubl. data) and isotopic shifts is intriguing. Both may be separate but related effects caused by paleoceanographic changes during the Maastrichtian (e.g., Frank and Arthur, 1999; Barrera and Savin, 1999; MacLeod and Huber, 2001).

Potential primary causes for the shift in $\delta^{18}O$ values include temperature, salinity, and seawater isotopic composition. Large regional changes in salinity seem unlikely for these sites because they are within a very large ocean basin, and possible global changes in seawater $\delta^{18}O$ seem to be contradicted by decreasing $\delta^{18}O$ values observed in correlative samples from the North Atlantic (MacLeod et al., 2000; MacLeod and Huber, 2002). If the shift seen on OJP is the result of temperature change, the ~0.5‰ increase suggests cooling of ≥2°C. In support of cooling, increases in $\delta^{18}O$ values across the Maastrichtian have been

documented in a variety of samples from widely distributed localities and independent evidence for widespread cooling is provided by floral, faunal, and biogeographic evidence (see data and references in Frank and Arthur, 1999; Barrera and Savin, 1999; MacLeod and Huber, 2001). If accurate, the temperature interpretation expands the documented area that experienced Maastrichtian cooling to the southwestern tropical and subtropical Cretaceous Pacific. The magnitude of the shift is similar to those reported for good to well-preserved planktonic foraminifers from Shatsky Rise and the Mid-Pacific Mountains (Barrera et al., 1997; Barrera and Savin, 1999) located north and east of OJP and Manihiki Plateau.

That a Late Cretaceous temperature signal may have survived in all these sections is remarkable. The samples are obviously lithified, and average $\delta^{18}O$ values vary by >2‰ among the sites. In addition, the most deeply buried and most highly lithified samples (Hole 807C) have $\delta^{18}O$ values that yield paleotemperature estimates that are most reasonable for planktonic carbonate in a tropical greenhouse ocean. On the other hand, the least lithified samples (Hole 288A) have $\delta^{18}O$ ratios that yield improbably cool paleotemperature estimates for this setting. The compositional uniformity within and among samples could make it difficult for burial diagenesis to completely obscure depositional trends, but it does not explain why the qualitatively least altered samples result in the apparently worst paleotemperature estimates, and vice versa. Planktonic foraminifers are relatively abundant in the samples from Hole 288A and, if those foraminifers largely represent deeper dwelling taxa, it could explain part of the difference, but only if the evidence for alteration is largely ignored.

The explanation we favor is that the OJP data set provides an example among sites (rather than downcore in a single site) of changes in the direction of diagenetic effects on $\delta^{18}O$ values with increasing burial depth (e.g., Schrag et al., 1992, 1995). Assuming that (1) $\delta^{18}O$ values of the bulk carbonate were initially low at all sites (because the carbonate precipitated dominantly in warm surface waters), (2) samples from Hole 288A are the least geochemically altered, and (3) samples from Hole 807C are the most altered, then $\delta^{18}O$ values must have first been shifted to higher values (Hole 288A) and then shifted back to lower values (Holes 317A to 1183A to 1186A to 289 to 807C, progressively more lithified). Under this model, the initial shift toward higher $\delta^{18}O$ values would represent early alteration/recrystallization in bottom waters/near-bottom pore waters that were cooler than contemporary surface waters—a process that may explain the cool tropics paradox (D'Hondt and Arthur, 1996; Pearson et al., 2001). The shift back toward low $\delta^{18}O$ values would represent late alteration and reflect increasing temperatures with increasing burial. Because samples in Hole 288A were never as deeply buried as samples at other sites, they only experienced the former, whereas alteration in Hole 807C coincidentally has resulted in $\delta^{18}O$ values that approach reasonable Late Cretaceous levels. Finally, alteration related to hydrothermal circulation and proximity to basalt crust seems to affect the oldest samples from Holes 1183A, 1186A, and 289A (Fig. **F3;** Table **T2**).

Surprisingly, the $\delta^{13}C$ signal provides less paleoceanographic insight than the $\delta^{18}O$ record. Values of $3‰_{VPDB}$ are reasonable for Late Cretaceous surface water, and the large number of samples in five (of six) holes with $\delta^{13}C \approx 3‰_{VPDB}$ suggests it approximates a background value. As with $\delta^{18}O$ values, Hole 288A represents one end-member of the

range of isotopic values observed. A relatively high abundance of deeper-dwelling thermocline taxa among the planktonic foraminifers in this hole coupled with changing taxonomic composition through the section could explain the difference, but this possibility has not been tested.

The large $\delta^{13}C$ excursion at or near the K/T boundary in Holes 289, 807C, 1183A, and 1186A (Fig. F3, F4) seems to be a diagenetic artifact. Studies on samples from Hole 807C suggested this feature might be primary and unusually well expressed at that site because of the expanded nature of that section (Corfield and Cartlidge, 1993; Corfield et al., 1993). However, the duration and magnitude of the excursion is quite unusual for the increasingly well documented K/T record, and the excursion is not consistently expressed among these six sites. Further, the limestones in the vicinity of the K/T boundary are partially silicified at several sites. Preferential cementation of the K/T boundary interval may explain why the boundary interval has been recovered more often in Pacific drilling than expected, given average recovery rates for the Upper Cretaceous and Paleogene. The $\delta^{13}C$ excursion in Holes 289, 807C, 1183A, and 1186A could be a manifestation of this selective alteration. This possibility seems more likely than unusual paleoenvironmental conditions during the K/T boundary interval in the tropical Pacific, especially since faunal patterns across the boundary at many Pacific sites seem consistent with the impact hypothesis.

CONCLUSIONS

Comparisons of $\delta^{18}O$ values among five sites from OJP and one site from Manihiki Plateau suggest that widespread Maastrichtian cooling affected these regions as well. These sites are farther south and west than other Maastrichtian tropical to subtropical Pacific sites. The $\delta^{18}O$ evidence for cooling appears to be a remarkably robust signal; it seems to have survived at all sites despite moderate to high degrees of lithification. The differences in average $\delta^{18}O$ values among sites matches the predicted pattern of initial alteration toward higher values and subsequent alteration toward lower values. In contrast to the systematic trends through the Maastrichtian in $\delta^{18}O$ values, $\delta^{13}C$ values seem to be relatively constant through the late Campanian and Maastrichtian. An excursion at or near the K/T boundary interval at four of the study sites is most likely the result of selective cementation of limestones in the boundary interval.

ACKNOWLEDGMENTS

We thank Tracy Frank, Cheryl Kelley, and Woody Wise for comments on the manuscript and Jim Ogg, Paul Sikora, and Paul Wilson for helpful discussions. Samples were provided by the Ocean Drilling Program (ODP). ODP is sponsored by the U.S. National Science Foundation (NSF) and participating countries under management of Joint Oceanographic Institutions (JOI), Inc. Funding for this study was provided by the U.S. Science Support Program.

REFERENCES

Andrews, J.E., Packham, G., et al., 1975. *Init. Repts. DSDP,* 30: Washington (U.S. Govt. Printing Office).

Barrera, E., and Savin, S.M., 1999. Evolution of Campanian–Maastrichtian marine climates and oceans. *In* Barrera, E., and Johnson, C.C. (Eds.), *Evolution of the Cretaceous Ocean-Climate System*. Spec. Pap.—Geol. Soc. Am., 332:245–282.

Barrera, E., Savin, S.M., Thomas, E., and Jones, C.E., 1997. Evidence for thermohaline-circulation reversals controlled by sea level change in the latest Cretaceous. *Geology,* 25:715–718.

Bergen, J.A., 2004. Calcareous nannofossils from ODP Leg 192, Ontong Java Plateau. *In* Fitton, J.G., Mahoney, J.J., Wallace, P.J., and Saunders, A.D. (Eds.), Origin and Evolution of the Ontong Java Plateau. Geol. Soc. Spec. Publ., 229:113-132.

Coffin, M.F., Lawver, L.A., and Gahagan, L.M., 1998. Atlas of paleogeographic reconstructions, PLATES progress report no. 215-0798. *Univ. Tex., Inst. Geophys. [Tech. Rep.],* 181:1–88.

Corfield, R.M., and Cartlidge, J.E., 1993. Whole-rock oxygen and carbon isotope stratigraphy of the Paleogene and Cretaceous/Tertiary boundary in Hole 807C. *In* Berger, W.H., Kroenke, L.W., Mayer, L.A., et al., *Proc. ODP, Sci. Results,* 130: College Station, TX (Ocean Drilling Program), 259–268.

Corfield, R.M., Sliter, W.V., Premoli Silva, I., Tarduno, J.A., Schmitt, R.A., Liu, Y.-G, Wise, S.W., Jr., Mao, S., Cartlidge, J.E., and Berger, W.H., 1993. Synthesis of Cretaceous/Tertiary boundary studies at Hole 807C. *In* Berger, W.H., Kroenke, L.W., Mayer, L.A., et al., *Proc. ODP, Sci. Results,* 130: College Station, TX (Ocean Drilling Program), 745–751.

D'Hondt, S., and Arthur, M.A., 1996. Late Cretaceous oceans and the cool tropic paradox. *Science,* 271:1838–1841.

Frank, T.D., and Arthur, M.A., 1999. Tectonic forcings of Maastrichtian ocean-climate evolution. *Paleoceanography,* 14:103–117.

Kroenke, L.W., Berger, W.H., Janecek, T.R., et al., 1991. *Proc. ODP, Init. Repts.,* 130: College Station, TX (Ocean Drilling Program).

MacLeod, K.G., Fullagar, P.D., and Huber, B.T., 2003. $^{87}Sr/^{86}Sr$ test of the degree of impact-induced slope failure in the Maastrichtian of the western North Atlantic. *Geology,* 31:311–314.

MacLeod, K.G., and Huber, B.T., 2001. The Maastrichtian record at Blake Nose (western North Atlantic) and implications for global palaeoceanographic and biotic changes. *In* Kroon, D., Norris, R.D., and Klaus, A. (Eds.), *Western North Atlantic Paleogene and Cretaceous Paleoceanography.* Geol. Soc. Spec. Publ., 183:111–130.

————, 2002. Warming in the subtropical Western Atlantic during Maastrichtian cooling: hot tropics and latitudinal temperature gradients. [paper presented at JOI/USSP and NSF, Cretaceous Climate–Ocean Dynamics: Future Directions for IODP workshop, Florissant, CO, July 2002] (Abstract) Available from World Wide Web: <http://cis.whoi.edu/science/GG/ccod/viewAbstracts.cfm?RefNumber=19725628>. [Cited 2003-05-10]

MacLeod, K.G., Huber, B.T., and Ducharme, M.L., 2000. Paleontological and geochemical constraints on changes in the deep ocean during the Cretaceous greenhouse interval. *In* Huber, B., MacLeod, K., and Wing, S. (Eds.), *Warm Climates in Earth History:* Cambridge (Cambridge Univ. Press), 241–274.

Mahoney, J.J., Fitton, J.G., Wallace, P.J., et al., 2001. *Proc. ODP, Init. Repts.,* 192 [CD-ROM]. Available from: Ocean Drilling Program, Texas A&M University, College Station TX 77845-9547, USA.

Mao, S., and Wise, S.W., Jr., 1993. Mesozoic calcareous nannofossils from Leg 130. *In* Berger, W.H., Kroenke, L.W., Mayer, L.A., et al., *Proc. ODP, Sci. Results,* 130: College Station, TX (Ocean Drilling Program), 85–92.

McArthur, J.M., Howarth, R.J., and Bailey, T.R., 2001. Strontium isotope stratigraphy: LOWESS version 3: best fit to the marine Sr-isotope curve for 0–509 Ma and accompanying look-up table for deriving numerical age. *J. Geol.,* 109:155–170.

Pearson, P.N., Ditchfield, P.W., Singano, J., Harcourt-Brown, K.G., Nicholas, C.J., Olsson, R.K., Shackleton, N.J., and Hall, M.A., 2001. Warm tropical sea surface temperatures in the Late Cretaceous and Eocene epochs. *Nature,* 413:481–487.

Schrag, D.P., DePaolo, D.J., and Richter, F.M., 1992. Oxygen isotope exchange in a two-layer model of oceanic crust. *Earth Planet. Sci. Lett.,* 111:305–317.

————, 1995. Reconstructing past sea surface temperatures: correcting for diagenesis of bulk marine carbonate. *Geochim. Cosmochim. Acta,* 59:2265–2278.

Schlanger, S.O., Jackson, E.D., et al., 1976. *Init. Repts. DSDP,* 33: Washington (U.S. Govt. Printing Office).

Zachos, J., Pagani, M., Sloan, L., Thomas, E., and Billups, K., 2001. Trends, rhythms, and aberrations in global climate 65 Ma to present. *Science,* 292:686–693.

Figure F1. Paleogeographic map for ~65 Ma (after Coffin et al., 1998) showing the approximate location of the sites examined in this study. Note, no Cretaceous samples were analyzed at Sites 1184 and 1185.

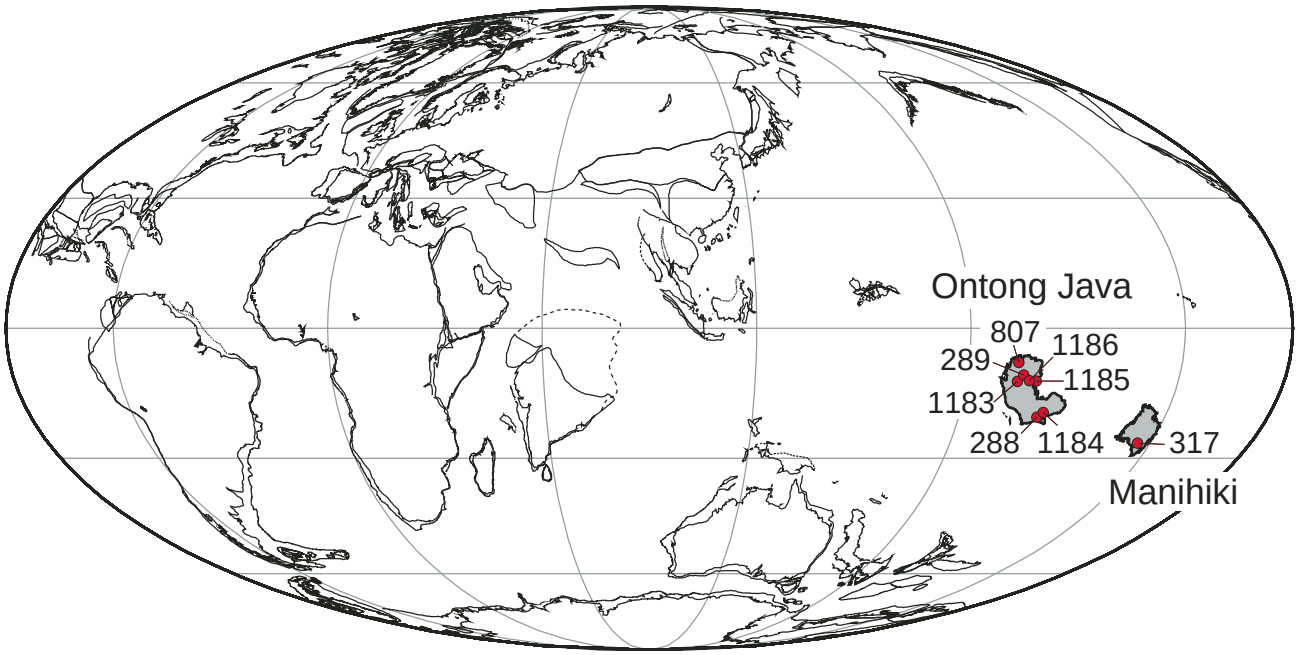

Figure F2. Age-depth plots based on $^{87}Sr/^{86}Sr$ analyses for samples from Holes 1183A and 1186A. Data are reported in **Bralower et al.** (this volume). See **"Materials and Methods,"** p. 2, for discussion of how $^{87}Sr/^{86}Sr$ data were converted to ages.

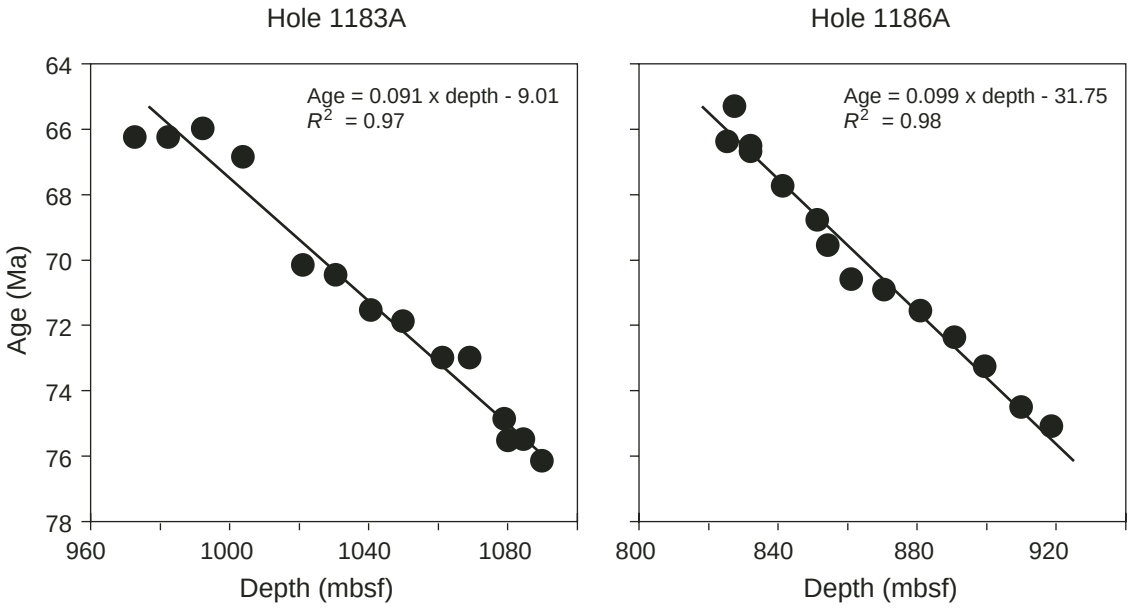

Figure F3. Plots of oxygen (solid symbols) and carbon (open symbols) isotopic values vs. depth for samples collected during Leg 192. Data for Holes 1185A and 1186A are on the same plot. Right bottom plot: Squares = data from Hole 1185A, and depth is shown on to the right; circles = data from Hole 1186A, and depth is shown to the left. All plots are at the same scale. Age estimates are based on nannofossil biostratigraphy from Bergen (2004); dotted lines show correlations among holes. The shaded box outlines the Campanian–Maastrichtian interval shown in Figure F4, p. 12. VPDB = Vienna Peedee belemnite.

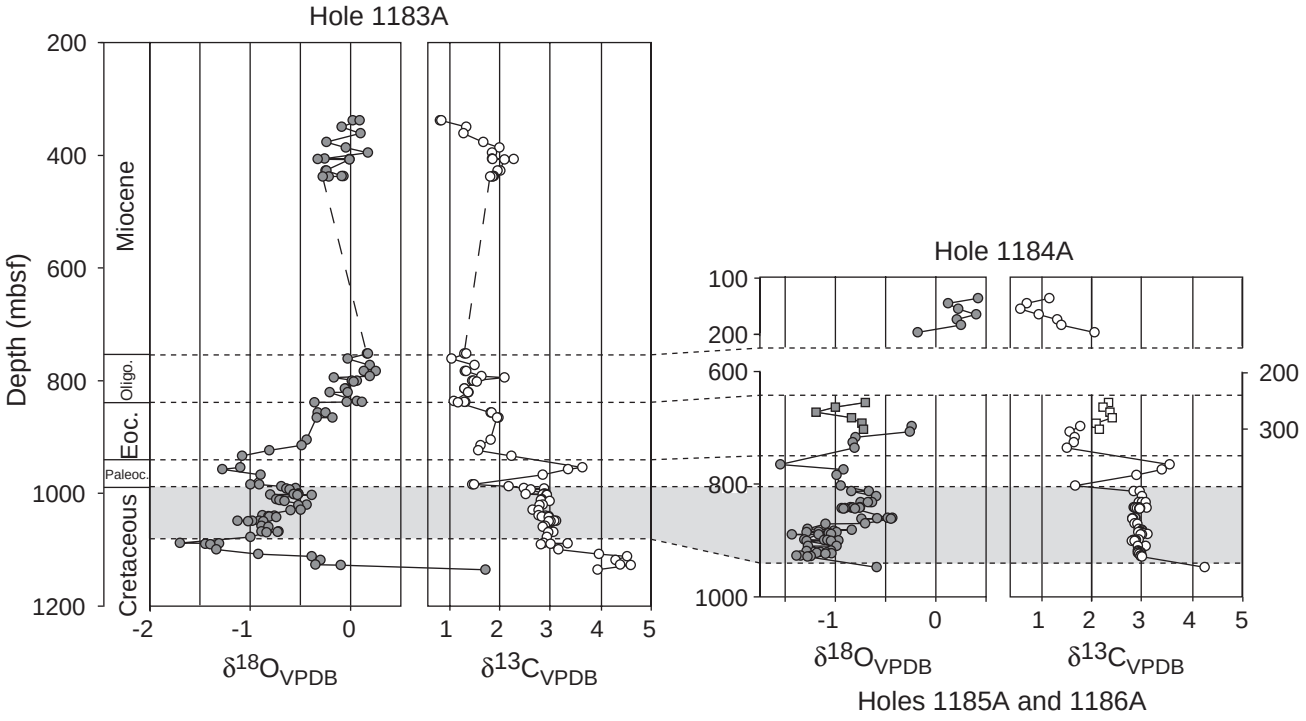

Figure F4. Oxygen isotopic and carbon isotopic plots of Campanian–Maastrichtian samples for the six sites at which this interval was sampled. Isotopic data are plotted against age based on the biostratigraphic tie points listed in Table T2, p. 14, and the Sr-based age model (Fig. F2, p. 10).

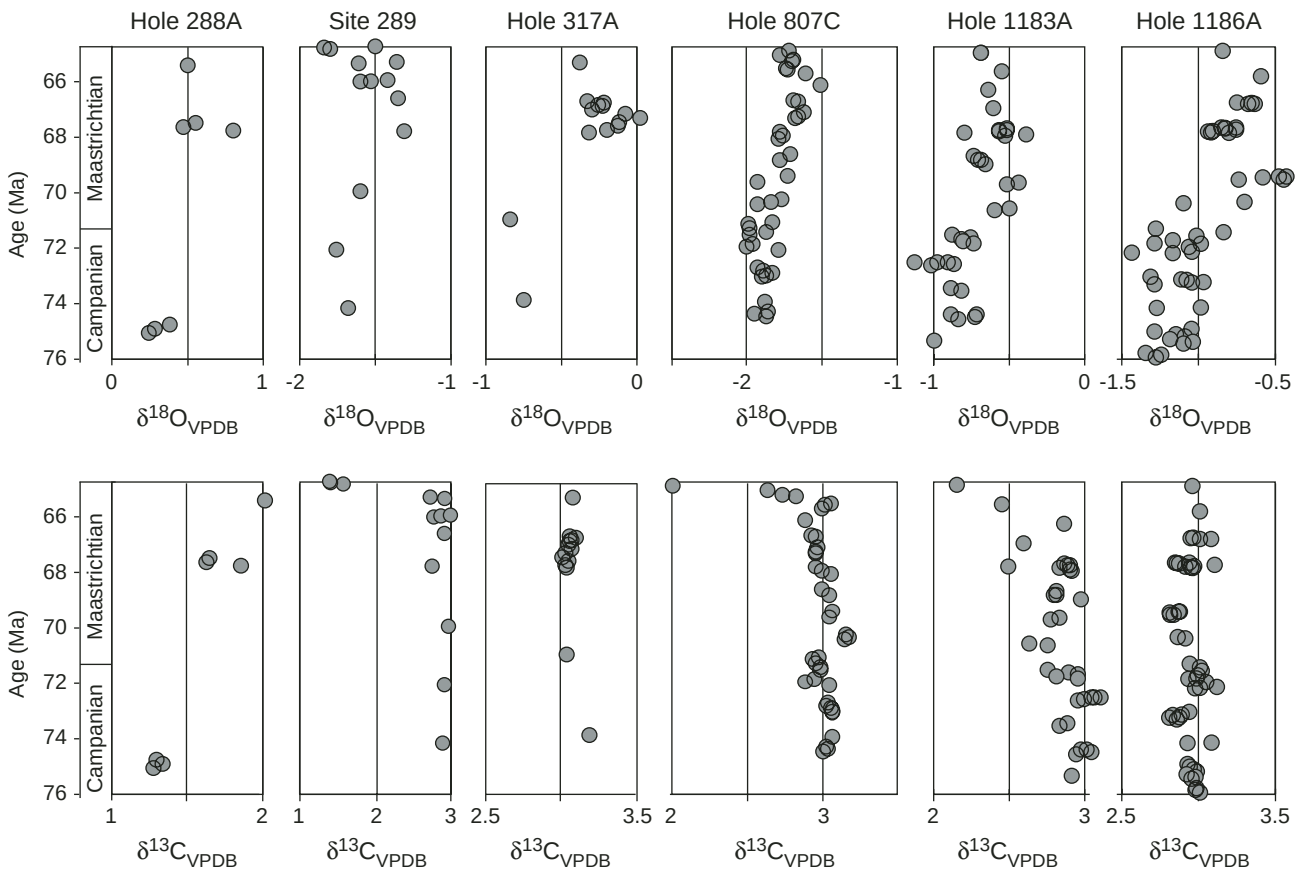

Table T1. Level of nannofossil datums used to correlate the six sites.

	Event depth (mbsf)					
Hole:	288A	289	317A	807C	1183A	1186A
K/T boundary		1146.8		1197.3	987.4	
FO *Micula murus*	<571.3	1166	<554.7	1262.3		
FO *Lithoquadratus quadratus*	609.8	1185	564.7	1315.2	995.36	812.88
FO *Arkhangelskiella cymbiformis*			573.2		1022.08	861.11
FO *Uniplanarius trifidus*	648.5	1213.5	582.5	1342.4	1069.29	908.83

Notes: FO = first occurrence. Depths for Holes 288A and 289 taken from Andrews, Packham, et al. (1975), depths for Hole 317A taken from Schlanger, Jackson, et al. (1976), depths for Hole 807C taken from Mao and Wise (1993), and depths for Holes 1183A and 1186A taken from Bergen (2004). K/T = Cretaceous/Tertiary.

Table T2. Stable isotope values of bulk samples, DSDP Holes 288A, 289, and 317A; ODP Holes 807C, 1183A, 1185A, and 1186A. (See table notes. Continued on next page.)

Core, section, interval (cm)	Depth (mbsf)	$\delta^{13}C_{VPDB}$	$\delta^{18}O_{VPDB}$
30-288A-			
9R-1, 54–56	571.54	2.02	0.50
10R-1, 129–131	610.29	1.65	0.55
10R-2, 59–61	611.09	1.63	0.47
10R-2, 127–129	611.77	1.86	0.80
11R-1, 123–125	648.23	1.30	0.38
11R-2, 54–56	649.04	1.34	0.28
11R-2, 128–130	649.78	1.28	0.24
30-289-			
122R-1, 129–131	1146.79	1.40	–1.00
122R-2, 54–56	1147.54	1.41	–1.34
122R-2, 130–132	1148.30	1.57	–1.30
123R-1, 40–42	1155.40	2.73	–0.86
123R-1, 110–112	1156.10	2.92	–1.11
124R-1, 84–86	1165.34	3.00	–0.92
124R-1, 138–142	1165.88	2.87	–1.03
124R-2, 11–13	1166.11	2.78	–1.10
125R-1, 118–120	1175.18	2.92	–0.85
126R-1, 114–116	1184.64	2.76	–0.81
127R-1, 131–133	1194.31	2.97	–1.10
128R-1, 123–129	1203.73	2.92	–1.26
129R-1, 115–117	1213.15	2.90	–1.18
131R-1, 110–112	1232.10	3.02	–1.37
131R-2, 17–19	1232.67	2.84	–1.41
131R-2, 101–103	1233.51	3.57	–1.24
131R-3, 21–23	1234.21	4.07	–0.59
131R-3, 91–93	1234.91	4.83	–0.30
33-317A-			
2R-1, 136–138	555.36	3.08	–0.38
3R-1, 44–46	563.94	3.06	–0.33
3R-1, 78–80	564.28	3.10	–0.22
3R-1, 130–132	564.80	3.07	–0.26
3R-2, 30–32	565.30	3.06	–0.23
3R-2, 76–78	565.76	3.05	–0.30
3R-2, 128–130	566.28	3.07	–0.08
3R-3, 26–28	566.76	3.03	0.02
3R-3, 78–80	567.28	3.01	–0.12
3R-3, 125–127	567.75	3.05	–0.13
3R-4, 28–30	568.28	3.03	–0.20
3R-4, 60–62	568.60	3.04	–0.32
5R-1, 130–132	577.30	3.04	–0.84
6R-1, 138–140	583.88	3.19	–0.75
130-807C-			
54R-4, 61–62	1193.91	1.63	–1.82
55R-1, 47–49	1197.37	1.99	–1.72
55R-4, 83–84	1202.23	2.63	–1.78
56R-1, 76–77	1207.36	2.73	–1.69
56R-2, 81–82	1208.91	2.82	–1.70
57R-1, 67–68	1216.97	3.05	–1.74
57R-2, 69–70	1218.49	3.01	–1.73
58R-1, 20–21	1222.70	2.99	–1.61
59R-3, 21–22	1235.41	2.88	–1.51
61R-1, 93–94	1252.43	2.92	–1.69
61R-2, 73–74	1253.73	2.95	–1.66
62R-2, 70–71	1263.40	2.96	–1.62
62R-3, 91–92	1265.11	2.95	–1.66
62R-4, 8–10	1265.79	2.95	–1.68
63R-2, 84–85	1271.64	2.95	–1.78
63R-2, 109–110	1273.39	2.99	–1.76
63R-3, 105–106	1274.85	3.05	–1.79
64R-1, 93–94	1281.43	2.99	–1.71
64R-3, 46–47	1283.96	3.04	–1.78
65R-1, 54–55	1290.64	3.06	–1.73
65R-3, 8–10	1293.18	3.04	–1.93
66R-1, 87–88	1300.67	3.15	–1.77
66R-2, 72–74	1302.02	3.17	–1.84
66R-3, 8–9	1302.88	3.14	–1.93
67R-1, 103–104	1310.53	2.97	–1.83
67R-2, 44–45	1311.38	2.93	–1.99
67R-3, 73–74	1313.17	2.95	–1.98
67R-4, 83–83	1314.77	2.98	–1.87
67R-5, 58–59	1316.02	2.98	–1.98
68R-1, 84–85	1319.94	2.94	–1.96
68R-2, 65–66	1321.25	2.88	–2.00
68R-3, 47–48	1322.57	3.04	–1.79
69R-1, 131–132	1330.11	3.03	–1.93
69R-2, 104–105	1331.34	3.02	–1.89
69R-3, 56–58	1332.36	3.05	–1.83
69R-4, 19–20	1333.49	3.06	–1.87
69R-4, 77–78	1334.07	3.06	–1.90
70R-5, 27–28	1344.67	3.06	–1.88
71R-1, 111–112	1349.11	3.02	–1.86
71R-2, 52–53	1350.02	3.03	–1.95
192-1183A-			
3R-1, 25–26	337.85	0.78	0.02
3R-1, 25–26	337.85	0.81	0.09
4R-2, 18–19	348.88	1.31	–0.09
5R-3, 48–59	360.28	1.25	0.10
7R-1, 33–34	376.23	1.65	–0.24
8R-1, 84–85	386.34	1.97	–0.05
9R-1, 25–26	395.35	1.82	0.17
10R-1, 85–86	405.55	1.82	–0.26
10R-1, 145–146	406.15	2.25	–0.01
10R-2, 45–46	406.65	1.83	–0.33
10R-2, 131–132	407.51	2.07	–0.01
12R-3, 45–46	427.35	1.99	–0.25
12R-3, 45–46	427.35	1.93	–0.24
13R-3, 9–10	436.59	1.86	–0.07
13R-3, 9–10	436.59	1.84	–0.09
14R-CC, 9–10	438.00	1.83	–0.22
14R-CC, 9–10	438.00	1.78	–0.28
15R-1, 86–87	752.86	1.27	0.16
15R-1, 86–87	752.86	1.31	0.17
16R-1, 46–47	761.56	1.01	–0.03
17R-2, 80–81	773.10	1.47	0.19
18R-3, 15.5–16.5	783.66	1.28	0.25
18R-3, 15.5–16.5	783.66	1.31	0.13
19R-2, 83–84	792.43	1.61	0.19
19R-4, 19–20	794.79	2.07	–0.17
20R-1, 131–132	801.01	1.43	0.06
20R-1, 131–132	801.01	1.45	0.01
20R-3, 6–7	802.76	1.52	0.03
21R-4, 112–113	814.92	1.27	–0.05
21R-4, 112–113	814.92	1.27	–0.06
22R-CC, 4–5	821.00	1.35	–0.03
22R-CC, 4–5	821.00	1.34	–0.21
23R-6, 68–69	836.78	1.06	0.06
24R-1, 62–63	838.82	1.29	0.11
24R-1, 62–63	838.82	1.27	–0.04
24R-CC, 6–7	839.00	1.14	–0.36
26R-CC, 14–15	857.00	1.79	–0.33
26R-CC, 14–15	857.00	1.81	–0.25
27R-CC, 18–19	866.60	1.95	–0.18
27R-CC, 18–19	866.60	1.92	–0.34
31R-1, 27–28	905.37	1.79	–0.44
32R-1, 77–78	915.47	1.59	–0.49
33R-1, 41–42	924.71	1.55	–0.81
34R-1, 71–72	934.61	2.21	–1.08
36R-2, 61–62	955.21	3.62	–1.10
36R-4, 87–88	958.47	3.34	–1.28
37R-4, 67–68	967.87	2.83	–0.90
39R-3, 45–46	985.45	1.43	–1.00
39R-3, 45–46	985.45	1.46	–0.91

Table T2 (continued).

Core, section, interval (cm)	Depth (mbsf)	$\delta^{13}C_{VPDB}$	$\delta^{18}O_{VPDB}$
39R-5, 60–61	988.60	2.15	–0.69
40R-1, 39–40	992.09	2.45	–0.55
40R-1, 119–120	992.89	2.86	–0.64
40R-2, 100–101	994.20	2.59	–0.61
41R-1, 7–8	1001.47	2.86	–0.52
41R-1, 73–74	1002.13	2.90	–0.52
41R-1, 74–75	1002.14	2.88	–0.57
41R-1, 120–121	1002.60	2.49	–0.57
41R-2, 17–18	1003.07	2.83	–0.80
41R-2, 80–81	1003.70	2.90	–0.39
41R-2, 118–119	1004.08	2.91	–0.53
42R-1, 30–31	1011.40	2.81	–0.74
42R-2, 26–27	1012.86	2.81	–0.69
42R-2, 28–29	1012.88	2.79	–0.71
42R-3, 30–31	1014.40	2.97	–0.66
43R-1, 29–30	1021.09	2.83	–0.44
43R-1, 98–99	1021.78	2.77	–0.52
44R-1, 9–10	1030.49	2.63	–0.50
44R-1, 79–80	1031.19	2.75	–0.60
45R-1, 6–7	1040.06	2.75	–0.88
45R-1, 99–100	1040.99	2.89	–0.76
45R-2, 19–20	1041.69	2.95	–0.82
45R-2, 95–96	1042.45	2.81	–0.81
45R-3, 29–30	1043.29	2.95	–0.74
46R-1, 42–43	1050.02	3.04	–1.13
46R-1, 43–44	1050.03	3.10	–0.91
46R-1, 43–44	1050.03	3.06	–0.98
46R-1, 115–116	1050.75	2.99	–0.87
46R-2, 12–13	1051.22	2.95	–1.02
47R-1, 21–22	1059.41	2.88	–0.89
47R-1, 121–122	1060.41	2.83	–0.82
48R-1, 9–10	1068.89	2.97	–0.89
48R-1, 10–11	1068.90	3.01	–0.72
48R-1, 113–114	1069.93	3.04	–0.73
48R-2, 31–32	1070.61	2.94	–0.84
49R-CC, 14–15	1078.50	2.91	–1.00
50R-1, 138–139	1089.58	2.85	–1.70
50R-2, 81–82	1090.51	3.33	–1.31
50R-2, 113–114	1090.83	2.99	–1.45
50R-3, 32–33	1091.52	2.79	–1.40
51R-3, 13–14	1101.03	3.14	–1.34
52R-1, 140–141	1108.90	3.95	–0.92
52R-4, 117–118	1113.17	4.51	–0.39
53R-2, 83–84	1119.53	4.28	–0.30
54R-1, 66–67	1127.46	4.37	–0.35
54R-2, 29–32	1128.59	4.58	–0.10
55R-1, 8–9	1136.58	3.92	1.34
192-1184A-			
2R-1, 51–52	134.92	1.16	0.42
3R-1, 35–36	144.35	0.71	0.12
4R-1, 42–43	154.12	0.58	0.22
5R-1, 38–39	163.68	0.95	0.40
6R-1, 29–30	173.19	1.32	0.21
7R-1, 39–40	182.89	1.40	0.25
8R-3, 89–90	195.69	2.06	–0.18
192-1185A-			
2R-2, 59–61	252.69	2.35	–0.70
3R-1, 31–32	260.51	2.24	–1.00
4R-1, 24–26	270.04	2.37	–1.19
5R-1, 26–27	279.76	2.42	–0.84
6R-1, 8–9	289.18	2.10	–0.74
7R-1, 93–94	299.73	2.16	–0.72
192-1186A-			
2R-1, 7–8	697.47	1.78	–0.24
3R-1, 29–30	707.19	1.57	–0.26
4R-1, 69–71	717.19	1.67	–0.80
5R-1, 47–49	726.57	1.65	–0.83
6R-CC, 5–6	735.75	1.51	–0.81
9R-1, 102–103	765.62	3.56	–1.55
10R-1, 69–70	774.89	3.40	–0.92
11R-1, 86–87	784.76	2.90	–0.99
13R-1, 28–29	803.38	1.68	–0.95
14R-CC, 1–2	812.71	2.84	–0.67
14R-CC, 4–6	812.74	2.96	–0.84
15R-CC, 1–2	822.31	3.01	–0.60
16R-1, 40–42	832.40	2.97	–0.75
16R-1, 62–63	832.62	2.95	–0.66
16R-1, 87–89	832.87	3.01	–0.64
16R-CC	833.00	3.08	–0.68
17R-1, 22–24	841.92	2.84	–0.76
17R-1, 30–32	842.00	2.94	–0.85
17R-1, 52–53	842.22	2.86	–0.83
17R-1, 55–57	842.25	2.87	–0.83
17R-1, 110–112	842.80	3.10	–0.76
17R-2, 21–22	843.41	2.97	–0.91
17R-2, 27–29	843.47	2.91	–0.94
17R-2, 66–69	843.86	2.95	–0.92
17R-CC	844.00	2.96	–0.81
19R-1, 14–15	860.74	2.88	–0.48
19R-1, 17–18	860.77	2.87	–0.43
19R-1, 50–51	861.10	2.81	–0.59
19R-CC	862.00	2.84	–0.74
20R-1, 25–26	870.45	2.86	–0.70
20R-CC	871.00	2.91	–1.10
21R-1, 70–72	880.60	2.94	–1.28
21R-2, 58–60	881.98	3.01	–0.84
21R-3, 52–54	883.42	3.02	–1.02
21R-4, 73–75	885.13	2.99	–1.17
21R-5, 32–34	886.22	2.98	–1.29
21R-5, 55–57	886.45	2.93	–0.99
21R-6, 24–26	887.64	3.05	–1.07
21R-CC	889.50	3.12	–1.05
22R-1, 35–37	889.85	3.01	–1.44
22R-CC	890.00	2.98	–1.17
23R-1, 106–109	900.16	2.89	–1.11
23R-1, 119–121	900.29	2.83	–1.08
23R-2, 49–51	901.09	2.88	–0.97
23R-2, 70–72	901.30	2.81	–1.05
23R-CC	902.00	2.86	–1.29
24R-2, 65–68	910.85	3.08	–0.99
24R-2, 83–86	911.03	2.93	–1.27
25R-1, 74–76	919.04	2.93	–1.05
25R-2, 27–29	920.07	2.94	–1.29
25R-2, 128–130	921.08	2.97	–1.15
25R-3, 66–68	921.96	2.99	–1.09
25R-4, 18–20	922.98	2.92	–1.19
25R-4, 115–117	923.95	2.98	–1.04
25R-5, 30–32	924.60	2.95	–1.10
26R-1, 21–22	928.21	2.98	–1.35
26R-1, 22–23	928.22	3.00	–1.39
26R-1, 83–84	928.83	2.98	–1.25
26R-2, 35–36	929.85	3.01	–1.28
28R-1, 135–136	948.55	4.26	–0.59

Notes: Values are reported in delta notation relative to the Vienna Peedee belemnite (VPDB) standard. External precision is <0.03 for $\delta^{13}C$ and <0.05 for $\delta^{18}O$ (1 σ standard deviation).